High Resolution ITU-R Cloud Attenuation Model for Satellite Communications in Tropical Region

Feng Yuan, *Student Member, IEEE*, Yee Hui Lee, *Senior Member, IEEE*, Yu Song Meng, *Member, IEEE*, Shilpa Manandhar, *Student Member, IEEE*, and Jin Teong Ong

***Abstract*— In this paper, the precipitable water vapor (PWV) data from GNSS (Global Navigation Satellite System) is introduced into the ITU-R cloud attenuation model for higher temporal and spatial resolution for the tropical region. The revised model incorporates PWV value for estimation of the cloud integrated liquid water content (ILWC), and then determine the cloud attenuation. In this study, ILWC along the propagation path is obtained by processing radiosonde vertical profile using the combination of water vapor pressure cloud detection model and the Salonen and Uppala liquid water density model. From the analysis of 2-years radiosonde data from 8 sites within the tropical region, the results show that the ILWC along the path can be approximated by a power function relationship with the PWV. The estimated cloud attenuation using the improved model is compared with the values calculated using the ITU-R model and the cloud attenuation derived from a Ka-band beacon data. The results show that the proposed model is in good agreement with the ITU-R model at high percentage of time exceedance for the thin layer of stratus clouds and matches well with cloud attenuation suffered from beacon signal at low percentage of time exceedance for the thick layer of cumulonimbus clouds.**

***Index Terms*—cloud attenuation, precipitable water vapor, satellite communication, radiosonde, and propagation**

I. Introduction

As the frequency spectrum becomes crowded and the demand for high data transmission rates increases, high frequency bands such as Ka-band and Q/V-bands are becoming increasingly interesting for satellite service operators [1]. Several fading impairments [1-3], such as precipitation attenuation, cloud attenuation, gaseous absorption, melting layer attenuation, and tropospheric scintillation, affect the Earth-to-Space and Space-to-Earth systems. With the increase in operating frequency, not only rain attenuation but also cloud attenuation becomes important for the satellite system design and operation. This is especially so for low margin systems such as VSATs (Very Small Aperture Terminals) and USATs (Ultra Small Aperture Terminals).

For the tropical region, the situation is severe due to the high-probability of occurrence of convective rain when the rainfall rate can reach up to 150 mm/hr and occurrence of cumulonimbus clouds [4] with heavy liquid water content over a large vertical extent. Therefore, convective rain and cumulonimbus cloud degrade the performance of satellite systems in the tropical region significantly.

From literature, rain attenuation in the tropical region has been extensively studied [5-6]. However, the cloud caused attenuation in the tropical region is less investigated. There are several cloud attenuation prediction models in the literature [7-15]. However, these models are mainly developed and evaluated using data collected in temperate countries. In their works, Altshuler *et al.* [7] and Dintelmann *et al.* [8] attempted to apply regression technique on surface meteorological parameter (i.e., surface humidity) to estimate cloud attenuation. Later in 1991, Salonen and Uppala [9] proposed to use the radiosonde vertical profile to detect the cloud vertical structure and then integrate the cloud liquid water content within the cloud layers to estimate the cloud attenuation. Owing to the microphysical concepts of the Salonen and Uppala (SU) model, it was adopted by the ITU-R Recommendation P.840-7 [10]. In 1997, a new approach to estimate cloud attenuation was proposed by Dissanayake *et al.* [11-12]. They categorized the clouds into four different types (cumulonimbus, cumulus, nimbostratus, and stratus) using average cloud properties such as vertical/horizontal extend and cloud water content. The respective cloud attenuations can then be calculated using the cloud water content where a best-fit log-normal relationship for cloud attenuation distribution was used.

Recently, Luini and Capsoni have proposed a methodology [13] to generate high-resolution three-dimensional fields of the cloud liquid water content and they discussed about scaling cloud attenuation among links with different elevations [14]. In 2017, Lyras *et al.* [15] proposed a stochastic dynamic model for generating integrated liquid water content (ILWC) fields by incorporating the spatial and temporal behavior of ILWC. After

Manuscript received May 2018. This work was supported in part by the Defence Science and Technology Agency, Singapore.

F. Yuan, Y. H. Lee, and S. Manandhar are with the School of Electrical and Electronic Engineering, Nanyang Technological University, 50 Nanyang Avenue, Singapore 639798 (e-mail: yuan0053@e.ntu.edu.sg, eyhlee@ntu.edu.sg).

Y. S. Meng is with the National Metrology Centre, Agency for Science, Technology and Research (A*STAR), 1 Science Park Drive, Singapore 118221 (e-mail: ysmeng@ieee.org, meng_yusong@nmc.a-star.edu.sg).

J. T. Ong is with the C2N Pte. Ltd., Singapore 199098.

classifying the cloud types and applying Rayleigh approximation (adopted in ITU-R P.840-7), they proposed a cloud attenuation model for frequencies above Ka-band up to the optical range.

It is well-known that water vapor plays an important role for the hydrologic cycle on Earth [16]. When the amount of water vapor is saturated at a certain temperature, it will condense to form clouds. Therefore, in this paper as a continuation of [17, 18], we will study the correlation between the amount of ILWC and that of precipitable water vapor (PWV), and then propose an improved approach for determining the cloud attenuation accurately in the tropical region.

In the following, Section II provides a review of cloud attenuation models, and discusses different approaches to calculate the cloud liquid water content and then cloud attenuation. The meteorological data (radiosonde profiles and PWV data) and beacon signal data used for the proposed cloud attenuation model are introduced in Section III. Section IV presents the methodology for determining the relationship between ILWC and PWV. The relationship is then used to improve the temporal and possibly spatial resolution of the ITU-R model in Section V. Performance evaluation of the proposed model is also presented in this section. Finally, a summary of the findings is given in Section VI.

II. Review of Cloud Attenuation Models

This section presents a review of several typical empirical cloud attenuation models in the literature, namely Altshuler and Marr model [7], Salonen and Uppala model [9], ITU-R model [10] and DAH model [11].

A. Cloud Attenuation Models

1) Altshuler and Marr Model

Altshuler and Marr [7] proposed a cloud attenuation model by applying surface meteorological variable in two conditions, i.e., complete cloud cover and partial cloud cover. For complete cloud cover, the cloud attenuation A_c

$$A_c = \left(-0.0242 + 0.00075\lambda + \frac{0.403}{\lambda^{1.15}}\right)(11.3 + \rho_s)D(\theta) \quad (1)$$

where λ is the wavelength in millimeters, ρ_s is the surface absolute humidity in g/m^3, and $D(\theta)$ is the distance through the attenuating layer as shown in (2),

$$D(\theta) = \begin{cases} csc\theta, & \theta > 8^\circ \\ [(a_e + h_e)^2 - a_e^2 cos^2\theta]^{1/2} - a_e sin\theta, & \theta \le 8 \end{cases} \quad (2)$$

where θ is the elevation angle, a_e is the effective earth radius $= 8497\ (km)$, and h_e is the effective height of the attenuating layer $= 6.35 - 0.302\rho_s\ (km)$.

For partial cloud cover, the mixed cloud attenuation A_m is estimated to be

$$A_m = 0.85A_c. \quad (3)$$

2) Salonen and Uppala Model

Salonen and Uppala [9] proposed another method to estimate the cloud attenuation by using radiosonde profile, with consideration of vertical water profile and cloud extent. They firstly developed a critical humidity function to detect different cloud layers as shown in (4),

$$RH_c = 1 - \alpha \cdot \sigma(1 - \sigma)[1 + \beta(\sigma - 0.5)] \quad (4)$$

where $\alpha = 1.0$ and $\beta = \sqrt{3}$; σ is the ratio of the pressure at the measured level and on the surface. If the measured humidity is higher than RH_c at the same pressure level, the considered level is in a cloud.

Then the liquid water density in g/m^3 within the cloud layer can be calculated by applying the expression in (5):

$$w = \begin{cases} w_0(1 + cT)\left(\frac{h_c}{h_r}\right)p_w(T) & T \ge 0^\circ C \\ w_0 e^{cT}\left(\frac{h_c}{h_r}\right)p_w(T) & T < 0^\circ C \end{cases} \quad (5)$$

where T is the temperature in ˚C, h_c is the height from the cloud base in meter, $w_0 = 0.17\ (\mathrm{g}/m^3)$, $c = 0.04\ (1/^\circ\mathrm{C})$ and $h_r = 1500\ (m)$. The cloud liquid water fraction, $p_w(T)$, is defined in (6):

$$p_w(T) = \begin{cases} 1 & T > 0^\circ\mathrm{C} \\ 1 + \frac{T}{20} & -20^\circ\mathrm{C} < T \le 0^\circ\mathrm{C} \\ 0 & T \le -20^\circ\mathrm{C} \end{cases} \quad (6)$$

The cloud attenuation can be calculated by integrating the specific attenuation γ_c(dB/km) along the path,

$$\gamma_c = \frac{0.819fw}{\varepsilon''(1+\eta^2)} \quad (7)$$

where f is the frequency in GHz, w is the cloud liquid water density in g/m^3, and $\eta = (2 + \varepsilon')/\varepsilon''$where ε' and $\varepsilon''$are the real and imaginary parts of the permittivity of water.

3) DAH Model

Later in 1997, by taking into consideration the different cloud types with different properties, DAH Model [11] was developed based on the liquid water content and the vertical and horizontal extent of four cloud types. Using the average cloud properties specified in Table I with the assumption of statistical distribution of cloud attenuation following a log-normal probability law, the specific attenuation γ_c (dB/km) for each cloud type i can be calculated as follows

$$\gamma_c = 0.4343\left(\frac{3\pi\nu}{32000\lambda\rho}\right)Im\left(\frac{1-\varepsilon}{2+\varepsilon}\right) \quad (8)$$

where ν is the cloud liquid water content in g/m^3, ρ is the water density $= 1\ (\mathrm{g}/cm^3)$, and $\varepsilon = \varepsilon' - j\varepsilon''$.

TABLE I
Average cloud properties in DAH model

Cloud Type (i)	Vertical Extent (km) H_c	Horizontal Extent (km) L_c	Water Content (g/m^3) ν
Cumulonimbus (1)	3.0	4.0	1.0
Cumulus (2)	2.0	3.0	0.6
Nimbostratus (3)	0.8	10.0	1.0
Stratus (4)	0.6	10.0	0.4

The total zenith cloud attenuation A_c for each of the cloud types ($i = 1$ to 4) is given by the product of the specific attenuation and the vertical extent

$$A_c = \gamma_c H_c \quad (9)$$

where H_c is the cloud vertical extent in kilometers. For the slant path, the cloud shape is assumed to be a vertical cylinder having the vertical and horizontal dimensions (H_c and L_c) in Table I.

After arranging the four cloud types in rank order, the cloud attenuation distribution curve A_c is

$$P(A > A_c) = \frac{P_0}{2} erfc\left(\frac{lnA - ln\bar{A}_c}{\sqrt{2}\sigma_c}\right) \quad (10)$$

where $P(A > A_c)$ is the probability of cloud attenuation A_c not exceeding A, P_0 is the probability of cloud attenuation being present, $erfc$ denotes the complementary error function, $\bar{A}_c$ is the mean value of A_c, and σ_c is the standard deviation of A_c. The total cloud cover provides the conditional probability for cloud attenuation distribution. With the five points selected above (including the four cloud types and clear sky), the best fit log-normal relationship for cloud attenuation distribution is obtained using linear regression analysis.

4) ITU-R Model

Most recently, the updated version of ITU-R P.840-7 [10] recommendation applied the SU method [9] to European Centre for Medium-Range Weather Forecasts (ECMWF) derived vertical profiles and achieve the liquid water content and cloud attenuation in frequencies below 200 GHz. For ECMWF database, the data applied are from the radiosondes which are launched normally under no-rain conditions if possible. The ITU-R model provides an overall yearly digital map of the global statistics of atmospheric reduced cloud liquid water. To calculate the cloud attenuation according to recommendation ITU-R P.840-7 [10, 19]:

$$A_c = \frac{K_l(f, 273.15) \cdot L_{red}}{sin\theta} \quad (11)$$

where K_l ((dB/km) $\cdot \mathrm{g}/m^3$) is the specific attenuation coefficient that depends on the temperature of suspended water droplets (usually set to 0 ˚C) and on the transmission frequency, L_{red} (kg/m^2) is the total columnar content of reduced cloud liquid water, and θ is the elevation angle.

In ITU-R P.840-7, a new approach [20] to calculate the cloud attenuation along slant path is proposed based on local data. The slant path cloud attenuation, A_c, is:

$$A_c = \frac{K_l^*(f, 273.15) \cdot ILWC}{sin\theta} \quad (12)$$

where $ILWC$ (kg/m^2) is the total columnar content of liquid water (i.e., integrated liquid water content as mentioned previously), K_l^* ((dB/km) $\cdot \mathrm{g}/m^3$) is the specific attenuation coefficient derived for local collected liquid water content data.

B. Model Comparison and Analysis

In a summary of the cloud attenuation models, it is found that Altshuler and Marr model requires complete/partial cloud coverage information. This is difficult to obtain during applications. The SU model applies radiosonde vertical profiles which can have a better vertical resolution, however, due to the low temporal and spatial resolution (typically 2 times per day from a single location of the meteorological service), it is difficult to determine the cloud attenuation at none-weather-balloon-launching times and sites. Owing to its strong microphysical theory, the SU model was applied in the ITU-R P.840-7 recommendation with a slightly better temporal resolution (4 times per day) by using the EMCWF. The DAH model utilizes the properties (water content, horizontal/vertical extent) of four types of cloud. However, they assumed that statistical distribution of cloud attenuation follows a log-normal probability law and that there is no overlap between occurrence probabilities of the cloud types. This makes the DAH model less accurate.

In addition, all these models were developed and evaluated using data collected in the temperate region and therefore has limited application to the tropical region [17]. Of these models, the ITU-R model is the most promising one, since it is based on 40 years of vertical atmospheric profiles statistics for the calculation of cloud attenuation. However, this model (i.e., ITU-R model) only provides statistics of cloud attenuation and it also lacks spatial resolution. Therefore, it is of great interest to propose a high spatial resolution cloud attenuation model. and will be the focus of this paper.

III. Data Description

Three types of data are used for the study of cloud attenuation in the tropical region; the radiosonde data, the GNSS (Global Navigation Satellite System) data and the Ka-band beacon receiver data from Wideband InterNetworking engineering test and Demonstration Satellite (WINDS).

A. Radiosonde Data

Radiosonde data are used to calculate the ILWC along the propagation path and are acquired from an online database provided by Department of Atmospheric Science, University of Wyoming [21]. The data is collected twice per day at a point location. The vertical resolution of the radiosonde data is around 200 m. The relative humidity, altitude, and temperature data from radiosonde are used to estimate the cloud vertical structure and to calculate the liquid water content in this work.

In order to examine the reliability of the cloud attenuation model for applications in the tropical region, radiosonde data from 8 tropical stations are acquired from the online database. For each station, 2 years of data, 2013 and 2014 are used; this is a total of about 16 years of data. The 8 stations are chosen to be within ±23˚ latitude and with a collocated IGS station within 50 km, the 8 stations with their corresponding locations are given in Table II.

B. GNSS Data

PWV values derived from GNSS data are used to estimate the ILWC. Determination of PWV values are based on the delay incurred to the signals travelling from a GNSS satellite to a ground receiver. The total delay along the zenith path is called as zenith total delay, ΔL_T^o. It can be partitioned into two parts: zenith hydrostatic delay, ΔL_h^o and zenith wet delay, ΔL_w^o. ΔL_h^o depends mainly on the surface pressure (P_s) [22] as show in the following:

$$\Delta L_h^o = (2.2779 \pm 0.0024)\frac{P_s}{f(L_a, H)} \quad (13)$$

$$f(L_a, H) = 1 - 0.00266\cos(2 \cdot L_a) - 0.00028H \quad (14)$$

where L_a is the latitude and H(km) is the height of the station. ΔL_w^o is a function of the atmospheric water vapor profile as follows:

$$\Delta L_w^o = 10^{-6}\left[(17 \pm 10)\int_0^\infty \frac{e}{T_k}dz + (3.776 \pm 0.03) \times 10^5 \int_0^\infty \frac{e}{T_k^2}dz\right] \quad (15)$$

where e is the water vapor pressure, T_k is the air temperature in Kelvins and z is the interval of altitude acquired from radio sounding vertical profiles. In this work, GNSS Inferred Positioning SYstem-Orbit Analysis and Simulation Software (GIPSY-OASIS) [23] has been used for the computation of ΔL_w^o. The input data for GIPSY-OASIS software is the Receiver Independent Exchange (RINEX) files from IGS.

After the ΔL_w^o is computed, PWV values [22] are calculated using (16)

$$PWV = \frac{PI \cdot \Delta L_w^o}{\rho} \quad (16)$$

Here, ρ is the water density $= 1\ (\mathrm{g}/cm^3)$ and PI is the dimensionless conversion factor determined by (17) as follows [24]:

$$PI = \left[-1 \cdot \mathrm{sgn}(L_a) \cdot 1.7 \cdot 10^{-5}|L_a|^{h_{fac}} - 0.0001\right] \times \cos\left(\frac{DoY - 28}{365.25}2\pi\right) + [0.165 - (1.7 \cdot 10^{-5})|L_a|^{1.65}] + f_H \quad (17)$$

where h_{fac} for the northern hemisphere is 1.48 with $\mathrm{sgn}(L_a) = 1$ and for the southern hemisphere is 1.25 with $\mathrm{sgn}(L_a) = -1$. DoY is the day of year for which the PI values are to be calculated. f_H is negligible for stations from the low-altitude (H < 1 km) region and $f_H = -2.38 \cdot 10^{-9}H$ for stations from the high-altitude (H > 1 km) region.

Using this procedure, two-year (2013-2014) PWV data are calculated for the 8 collocated tropical IGS (International GNSS Service) stations as listed in Table II. The time resolution of GNSS PWV data is every 5 minutes.

C. Beacon Receiver System

Beacon signal from WINDS is continuously recorded with 516 samples per minute at the ground station located at Nanyang Technological University (NTU), Singapore, at the operating frequency of 18.9 GHz at left-hand circular-polarization. The WINDS is located at 143°E and has an elevation angle of 44.5˚.

For WINDS beacon signal processing, the rapid fluctuation due to tropospheric scintillation is removed using a 6th-order Butterworth filter at a cutoff frequency of 20 mHz. Since the amplifier gain of the Low-Noise-Block (LNB) down converter varies with temperature, the sliding window technique is applied.

To differentiate the cloud events from the rain events, the dual-polarized weather radar reflectivity data are used as references with the aid of weather station and the whole sky imager at NTU site. The dual-polarized weather radar is located at Changi airport (1.35ºN, 103.97ºE) and operates in the S-band at a frequency of 2.71 GHz. It performs a full volume scan every 5 minute with a maximum range of 120 km at 8 elevation angles (1˚, 1.5˚, 3˚, 5˚, 7.5˚, 10˚, 20˚, and 40˚). If the reflectivity is less than 20 dBZ, the event will be considered as cloud instead of rain [17]. After removing the rain attenuation and gaseous absorption, the cloud attenuation is estimated.

In this study, two consecutive years (2014 and 2015) beacon signal data are processed to determine the statistical cloud caused attenuation This complementary cumulative distribution function (CCDF) of cloud attenuation is used to compare and evaluate the results from the proposed high-resolution cloud attenuation model in the following.

IV. The Relationship Between PWV and ILWC

In order to form clouds, the condensation of water vapor is a necessary process, and therefore the relationship between the amount of water vapor suspended in the air and the liquid water content in cloud is highly correlated. For the ITU-R model, there is still unsatisfactory temporal resolution (4 times per day) and spatial resolution (often at more locations relative to radiosonde). Moreover, in the tropical region, there is also a decrease in accuracy at low percentage of time exceedance where cumulonimbus clouds with higher cloud attenuation is present [17]. The ground-based GNSS meteorology with high temporal (1 data per 5 minute) and spatial resolution is then a promising alternative solution, since its derived PWV values along the propagation path is a good indicator for high

TABLE II
Radiosonde stations with collocated IGS stations for tropical regions

Radiosonde Station ID	Height# of RS Station	Location of Radiosondes	Lat.	Lon.	IGS Station ID	Height of IGS Station	Distance*
MDSD	14.0 m	Caucedo De Las Amer, Dominican Republic	18.43˚N	69.88˚W	RDSD	26.51 m	4.79 km
TFFR	11.0 m	Le Raizet, Guadeloupe	16.26˚N	61.51˚W	ABMF	16.01 m	1.88 km
SOCA	13.0 m	Rochambeau, French Guiana	4.83˚N	52.36˚W	KOUG	141.63 m	43.02 km
WSSS	16.0 m	NEA Upper Air Observatory, Singapore	1.34˚N	103.89˚E	NTUS	71.91 m	23.37 km
WIII	8.0 m	Jakarta, Indonesia	6.11 ˚S	106.65˚E	BAKO	139.73 m	47.69 km
NFFN	18.0 m	Nadi Airport, Fiji	17.75˚S	177.45˚E	LAUT	31.81 m	15.73 km
YBTL	9.0 m	Townsville Aero, Australia	19.25˚S	146.76˚E	TOW2	30.19 m	31.10 km
NWWN	72.0 m	Noumea, New Caledonia	22.26˚S	166.45˚E	NRMD	99.93 m	5.04 km

#Height is above the sea level.
*Distance is between IGS station and Radiosonde (RS) station.

resolution remote sensing of ILWC.

For calculating the zenith ILWC, we need to detect the cloud layers and calculate the liquid water content within that specific cloud layer, and then integrate them along the path. For cloud detection in the tropical region, an accurate model for detecting cloud vertical structure, i.e. water vapor pressure (WVP) cloud detection model in [18] will be used. The model is proven to have a higher accuracy as compared to the SU cloud detection model in (4) for the tropical region.

In the WVP model, the spatial pressure of water vapor is calculated at each level using the following equation:

$$e = RH \times \exp(-37.2465 + 0.213166T_k - 2.56908 \times 10^{-4}T_k^2) \quad (18)$$

where e is the water vapor pressure in hPa, RH is the relative humidity in percentage, and T_k is the absolute temperature in degrees Kelvin.

The critical water vapor pressure for cloud detection in tropical region is in the form of [18]

$$e_c = 28.81 \cdot \exp(-0.0004363 \cdot Alt) \quad (19)$$

where Alt is the altitude in meters, and e_c is the critical water vapor pressure threshold in hPa. If the measured water vapor pressure is larger than the critical water vapor pressure threshold given in (19) at the same level, this level is assumed to be in cloud.

To calculate the zenith ILWC, (5) and (6) provided by SU model are applied to the cloud layers detected by the WVP model. The ILWC can be calculated twice per day at a point location due to the low radiosonde launching resolution. The PWV data from GNSS signal are recorded every 5 minutes. For comparison purposes, in order to match the temporal and spatial resolution, only the PWV data at radiosonde launching time are processed for the regression fitting analysis.

In order to achieve a relatively large database for tropical region in this study, the collocated IGS and radiosonde stations are selected if their physical location separation distance is less than 50 km as listed in Table II. The scatter plot of ILWC versus PWV for two-year (2013-2014) data from 8 different tropical stations listed in Table II is shown in Fig.1 (a). It can be observed that the range of PWV data measured from GNSS is from around 22 mm to 69 mm with most of data concentrated from 40 mm to 60 mm in the tropical regions [25]; while the ILWC calculated from radiosonde ranges from 0 mm to 4 mm, which are also similar with the values provided in Table I [11]. It is also observed that the ILWC along the same propagation path has an approximate power function relationship with the PWV in the tropical region.

However, there are also some outliers observed in Fig.1(a), which might be due to the physical location separation between the IGS stations and the radiosonde stations. Another reason might be due to the position drifting of radiosonde. It is found that position of a radiosonde can drift according to the winds direction and might go towards or away from the IGS stations. In addition, the zenith PWV values determined from GNSS signal is an average from GNSS data along different slant paths, which may mean that the zenith ILWC from radiosonde and the zenith PWV from GNSS are not for an exact same vertical path.

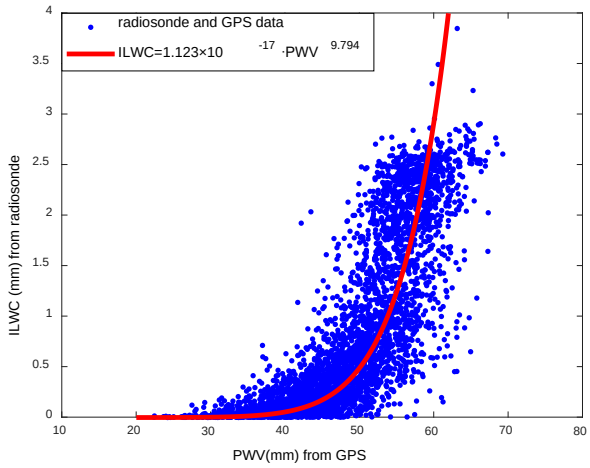

(a)

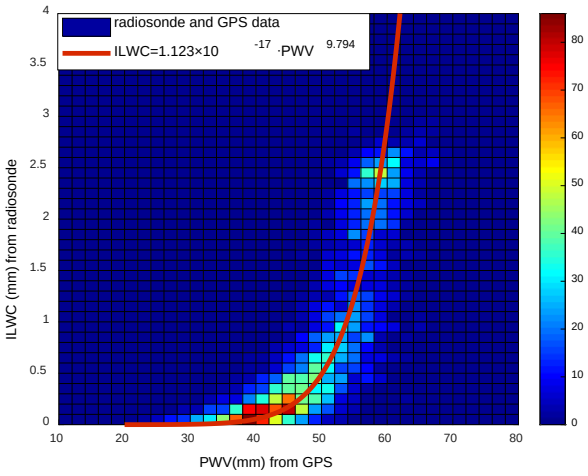

(b)

Fig. 1. Zenith ILWC processed from 8 radiosonde stations versus zenith PWV from the respectively collocated IGS station. (a) scatter plot, (b) density color image.

In order to understand distribution of data points, the density color image of ILWC versus PWV data is plotted in Fig.1(b). As shown in Fig.1(b), a large amount of ILWC is concentrated within the range of [0 0.5] mm, and these small ILWC is introduced by the thin stratus clouds. For the tropical region, the type of cloud that is frequently observed is the convective rain cloud (i.e., cumulus or cumulonimbus). Cumulonimbus clouds that occurs 22% of the time [17], are characterized as having a large vertical extent and are heavy with ILWC of more than 2.5 mm [12]. From the density color image in Fig.1(b), the correlation between ILWC and PWV is obvious.

The correlation function between ILWC and PWV is determined by applying regression fitting technique and can be express in (20),

$$ILWC = a \cdot PWV^b \quad (20)$$

where PWV is the precipitable liquid water in millimeter, and $ILWC$ is the integrated liquid water content in millimeter or kg/m^2. Through regression technique, empirical values for the two parameters a and b are derived to be 1.123×10^{-17} and

9.794.

Fig. 2 shows the CCDF plots of cloud integrated liquid water content ILWC calculated from the radiosonde data and the proposed model (20) with a =1.123 × $10^{-17}$and b = 9.794 for the year of 2013 and 2014. As shown in Fig. 2, around 90% of time, the two CCDF curves are in good agreement with each other. However, for the remaining 10% of time, the two curves diverse from each other significantly, the ILWC directly calculated from the radiosonde data saturates at around 3.84 kg/m^2, while for the ILWC calculated from the proposed model (20), it goes up to around 8.54 kg/m^2. The discrepancy might be due to the difference in path length use for the estimation of the ILWC. For radiosonde data, the ILWC is estimated up to a vertical space of 12 km or less from the ground station. For GNSS data, the ILWC is estimated from the ground receiver to GNSS satellite height. Taking GPS satellite as an example, its orbit height is around 20,200 km. In addition, there might be a lack of radiosonde measurements during extreme weather conditions such as thunderstorms [26].

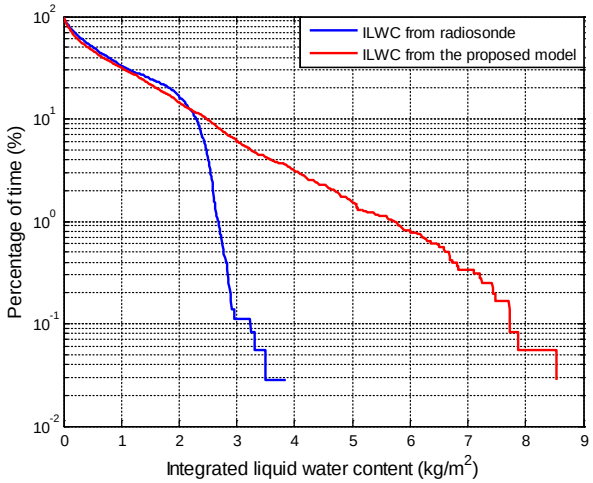

Fig. 2. CCDF of integrated liquid water content estimated from radiosonde and the proposed model.

By applying the ITU-R model, the attenuation caused by cloud ILWC of 3.84 kg/m^2 is around 1.76 dB for 18.9 GHz satellite beacon signal with an elevation angle of 44.8°, while for cloud ILWC of 8.54 kg/m^2, the corresponding cloud attenuation for the same satellite angle of link is around 3.91 dB. That is, the calculated cloud attenuation based on the radiosonde data using the ITU-R model saturates at around 1.76 dB which is much smaller as compared to the cloud attenuation of 4.2 dB at 0.01% of time experimentally determined from the WINDS beacon signal in tropical region as reported in [17]. This might be because the cloud ILWC is underestimated by SU liquid water density model for the tropical region. Therefore, in the next section, a relative accurate and high resolution ITU-R model is proposed by applying the proposed ILWC equation (20) to estimate the cloud attenuation for the tropical region.

V. Proposed High Resolution ITU-R Model and Its Performance Evaluation

A. *Proposed High Resolution ITU-R Model*

The ITU-R model is the promising method based on 40 years of vertical atmospheric profiles to calculate cloud attenuation. The relationship between PWV and ILWC can be utilized in (12) by replacing ILWC with PWV in (20). A high resolution ITU-R model for cloud attenuation A_c estimation is therefore proposed in this study in (21),

$$A_c = \frac{1.123 \times 10^{-17} \times K_l^*(f, 273.15) \cdot PWV^{9.794}}{sin\theta} \quad (21)$$

where f is the frequency in GHz and θ is the elevation angle of the slant path. The respective equation of K_l^* can be found in ITU-R P.840-7 [10]. This model is expected to have a much higher spatial resolution, limited only by the locations of GNSS receivers. In addition, it can be applied for the calculation of instantaneous cloud attenuation using the 5 minutes PWV data obtained from GNSS.

B. *Performance Evaluation*

To evaluate the performance of the proposed high resolution ITU-R model given in (21), comparisons with the existing ITU-R P.840-7 model, SU model and cloud attenuation derived from WINDS beacon signal is performed. This satellite-ground communication link operates at 18.9 GHz with an elevation angle of 44.5˚.

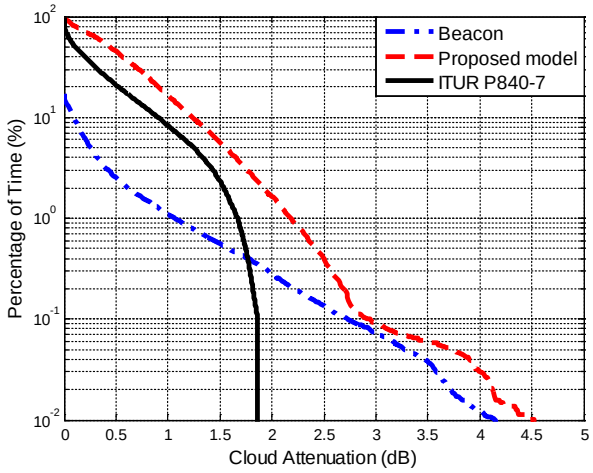

(a)

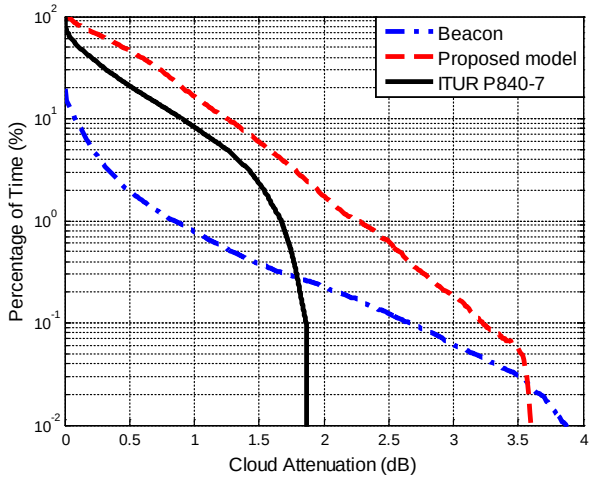

(b)

Fig. 3. CCDF of cloud attenuation estimated from the proposed model, derived from WINDS satellite beacon signal, SU model and ITU-R P.840-7 model for the year of (a) 2014 and (b) 2015.

In the comparison, the WINDS beacon signal from the year of 2014 and 2015 are processed using the method in [17], and the respective CCDFs are plotted in Fig. 3 (a) and (b). After processing the PWV data of 2014 and 2015, the cloud attenuation can be calculated by using (21) directly. For ITU-R P.840-7 model, after using the latitude and longitude of the respective location to find the distribution of liquid water content, the CCDF of cloud attenuation is also plotted in Fig. 3 (a) and (b).

In Fig. 3(a) and Fig. 3(b), the CCDFs of cloud attenuation for the year of 2014 and 2015 are plotted respectively. It can be observed that for the higher percentage of time exceedance (greater than 1%), the proposed method has slightly higher than the cloud attenuation obtained from the ITU-R method. The reason is because, the PWV derived from GNSS signal is the average of PWV values from several GNSS satellites which are in the line of sight as shown in Fig.4. Therefore, it will have a higher probability of detecting cloud layers and correspondingly the cloud caused attenuation. This is higher than a single propagation path obtained from the radiosonde or beacon signal. In addition, it should be noticed that the WVP cloud detection model has a better cloud detection rate compared to the one used in ITU-R model as we reported in [18].

For the cloud attenuation derived from WINDS beacon signal, at higher percentage of time exceedance (greater than 1%) where the attenuation is due to the thin layers of clouds, cumulative cloud attenuation is low. This is due to the fact that most of the thin cloud caused attenuation is missed since it is very difficult to process and estimate thin cloud caused attenuation from the beacon signal [17].

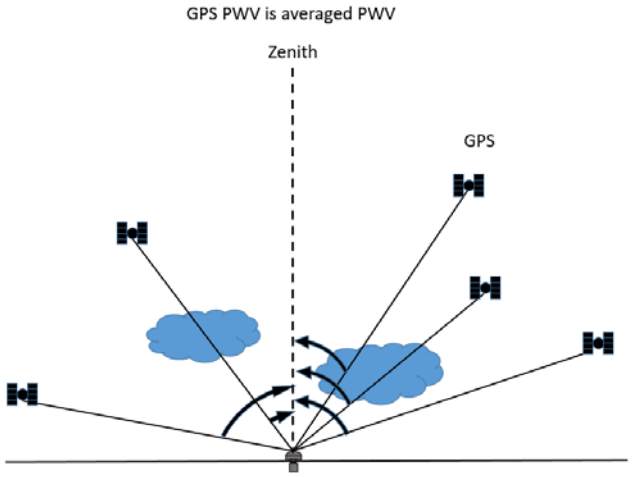

Fig. 4. Idea of zenith PWV determination.

Another interesting observation is that, at the lower percentage of time exceedance of less than 0.1%, the cloud attenuation estimated by the proposed model in (21) matches better with that derived from beacon signal, compared to the ITU-R model. The cloud attenuations reach more than 4 dB in 2014 and over 3.5 dB in 2015 at 0.01% of time. However, for the ITU-R model, the maximum cloud attenuation is only around 1.86 dB. It should be noted that the ITU-R is a global model and it applied the SU model derived from temperate region, which might not serve well for the tropical region. In addition, it is also discussed in [27] that severe weather conditions in the tropical region can result in much larger cloud attenuation at lower percentages of time exceedance especially for less than 0.1% of time.

Furthermore, it is found that there is less cloud attenuation determined by the proposed model for 2015 at the lower percentage of time exceedance. The main reason is that in the year of 2015, the El Nino climate dominated in Singapore, and the weather was warm and dry (less PWV).

VI. Conclusion

In this paper, an improved approach to estimate the cloud attenuation along the propagation path is proposed in this paper. The model is based on the correlation relationship between PWV and ILWC, which was determined from 2-year GNSS-PWV and radiosonde data collected from 8 tropical stations.

The estimated results of cloud attenuation using our proposed model are compared with those results from ITU-R model and beacon signal. The results show that the proposed model has a better performance for estimating cloud attenuation in tropical region at lower percentage of time exceedance. For the higher percentage of time exceedance, it slightly overestimates the cloud appearance percentage comparing with ITU-R model.

In general, investigation in this study shows that the proposed modified ITU-R model can be used for cloud attenuation estimation in tropical region with better spatial resolution and improved accuracy.

References

[1] A. D. Panagopoulos, P. M. Arapoglou, and P. G. Cottis, “Satellite communications at Ku, Ka, and V bands: propagation impairments and mitigation techniques,” *IEEE Commun. Surv. Tutor.*, vol. 6, no. 3, pp. 2–14, Oct. 2004.

[2] L. Luini, C. Riva, C. Capsoni, and A. Martellucci, “Attenuation in nonrainy conditions at millimeter wavelengths: Assessment of a procedure,” *IEEE Trans. Geosci. Remote Sens.*, vol. 45, no. 7, pp. 2150–2157, Jul. 2007.

[3] G. A. Siles, J. M. Riera, and P. Garcia-del-Pino, “Atmospheric attenuation in wireless communication systems at millimeter and THz frequencies,” *IEEE Antennas Propag. Mag.*, vol. 5, no. 1, pp. 48–61, Feb. 2015.

[4] F. Yuan, Y. H. Lee, and Y. S. Meng, “Comparison of radio-sounding profiles for cloud attenuation analysis in the tropical region,” in *Proc. IEEE Antennas Propaga. Soc. Int. Symp.*, Memphis, USA, pp. 259 –260, Jul. 2014.

[5] L. S. Kumar, Y. H. Lee, and J. T. Ong, “Truncated Gamma drop size distribution models for rain attenuation in Singapore,” *IEEE Trans. Antennas Propag.*, vol. 58, no. 4, pp. 1325–1335, Apr. 2010.

[6] J. X. Yeo, Y. H. Lee, and J. T. Ong, “Rain attenuation prediction model for satellite communications in tropical regions,” *IEEE Trans. Antennas Propag.*, vol.62, no. 11, pp. 5775–5781, Sep. 2014.

[7] E. Altshuler and R. Marr, “Cloud attenuation at millimeter wavelengths,” *IEEE Trans. Antennas Propag.*, vol. 37, no. 11, pp.1473–1479, Nov. 1989.

[8] F. Dintelmann and G. Ortgies, “Semiempirical model for cloud attenuation prediction,” *Electron. Lett.*, vol. 25, pp. 1479–1487, Oct. 1989.

[9] E. Salonen and S. Uppala, “New prediction method of cloud attenuation,” *Electron. Lett.*, vol. 27, no. 12, pp. 1106–1108, Jun. 1991.

[10] Rec. ITU-R P.840-7, Attenuation due to clouds and fog, 2017.

[11] A. Dissanayake, J. Allnutt, and F. Haidara, “A prediction model that combines rain attenuation and other propagation impairments along earth-

satellite paths," *IEEE Trans. Antennas Propag.*, vol. 45, no. 10, pp.1546 –1558, Oct. 1997.

[12] A. Dissanayake, J. Allnutt and F. Haidara, "Cloud attenuation modelling for SHF and EHF applications," *Int. J. Satell. Commun.*, vol. 19, no. 3, pp. 335–345, May 2001.

[13] L. Luini and C. Capsoni, "Modeling high-resolution 3-D cloud fields for earth-space communication systems," *IEEE Trans. Antennas Propag.*, vol. 62, no. 10, pp. 5190–5199, Oct. 2014.

[14] L. Luini and C. Capsoni, "Scaling cloud attenuation statistics with link elevation in earth-space applications", *IEEE Trans. Antennas Propag.*, vol. 64, no. 3, pp. 1089–1095, Mar. 2016.

[15] N. K. Lyras, C. I. Kourogiorgas, and A. D. Panagopoulos, "Cloud attenuation statistics prediction from Ka-Band to optical frequencies: integrated liquid water content field synthesizer," *IEEE Trans. Antennas Propag.*, vol. 65, no. 1, pp. 319–328, Jan. 2017.

[16] D. Ji and J. Shi, "Water vapor retrieval over cloud cover area on land using AMSR-E and MODIS," *IEEE J. Sel. Topics Appl. Earth Observ.*, vol. 7, no. 7, pp. 3105–3116, Jul. 2014.

[17] F. Yuan, Y. H. Lee, Y. S. Meng, J. X. Yeo, and J. T. Ong, "Statistical study of cloud attenuation on Ka-band satellite signal in tropical region," *IEEE Antennas Wireless Propag. Lett.* vol. 16, pp. 2018–2021, 2017.

[18] F. Yuan, Y. H. Lee, Y. S. Meng, and J. T. Ong, "Water vapor pressure model for cloud vertical structure detection in tropical region," *IEEE Trans. Geosci. Remote Sens*., vol. 54, no. 10, pp. 5875-5883, Oct. 2016.

[19] L. Luini, C. Riva, and C. Capsoni, "Reduced liquid water content for cloud attenuation prediction: the impact of temperature," *Electron. Lett.*, vol. 49, no. 20, pp. 1259 –1261, Sep. 2013.

[20] L. Luini and C. Capsoni, "Efficient calculation of cloud attenuation for earth-space applications," *IEEE Antennas Wireless Propag. Lett.*, vol. 13, pp. 1136-1139, 2014.

[21] Department of Atmospheric Science, University of Wyoming, http://weather.uwyo.edu/upperair/sounding.html

[22] G. Elgered, J. L. Davis, T. A. Herring, and I. I Shapiro, "Geodesy by radio interferometry: water vapor radiometry for estimation of the wet delay," *J. Geophys. Res.*, vol. 96, no. B4, pp. 6541–6555, Apr. 1991.

[23] S. Desai and W. Bertiger, "GIPSY/OASIS (GIPSY) overview and under the hood," Near Earth Tracking Systems and Applications Groups, JPL, California Institute of Technology, Mar. 2014.

[24] S. Manandhar, Y. H. Lee, Y. S. Meng, and J. T. Ong, "A simplified model for the retrieval of precipitable water vapor from GPS signal," *IEEE Trans. Geosci. Remote Sens*., vol. 55, no. 11, pp. 6245-6253, Nov. 2017.

[25] S. Manandhar, Y. H. Lee, and S. Dev, "GPS derived PWV for rainfall monitoring," *2016 IEEE Int. Geosci. Remote Sens. Symp. (IGARSS)*, Beijing, 2016, pp. 2170-2173.

[26] Vaisala, "Accuracy matters in radiosonde measurements," 2016, https://www.vaisala.com/sites/default/files/documents/Accuracy-Matters-in-Radiosonde-Measurements-White-Paper-B211548EN.pdf

[27] ITU-R, "Fascicle concerning the statistical distribution of integrated water vapour and liquid water contents given in Recommendations ITU-R P.836-4 and ITU-R P.840-4," 2013.